

Aharonov-Bohm Effect in Concentric Quantum Double Rings

Guang-Yin Chen,¹ Yueh-Nan Chen,^{2,3,*} and Der-San Chuu⁴

¹*Institute of Physics, National Chiao Tung University, Hsinchu 300, Taiwan*

²*Department of Physics, National Cheng Kung University, Tainan 701, Taiwan*

³*National Center for Theoretical Sciences, Tainan 701, Taiwan*

⁴*Department of Electrophysics, National Chiao Tung University, Hsinchu 300, Taiwan*

(Dated: June 25, 2018)

We propose a theoretical model to study the single-electron spectra of the concentric quantum double ring fabricated lately by self-assembled technique. Exact diagonalization method is employed to examine the Aharonov-Bohm effect in the concentric double ring. It is found the appearance of the AB oscillation in total energy depends on the strength of the screened potential. Variations of the energy spectra with the presence of coulomb impurities located at inner or outer ring are also investigated.

PACS numbers: 73.22.-f

Due to the presence of ring-like structures in the past two decades, observing Aharonov-Bohm (AB) effect¹ is no longer impossible. The first observation of AB effect in normal metal rings was reported by Webb *et al.*². On the theoretical side, Cheung *et al.*³ calculated the persistent currents and energy levels of the electron in a one-dimensional ring. Gap-like structure was found with the presence of impurities.

In addition to the metallic quantum rings, A. V. Chaplik⁴ in 1995 considered a semiconducting antidot under a strong magnetic field. It was found the tunnelings of the electron and hole around the antidot may result in a shift for each excitonic level. Römer and Raikh⁵ then found similar results by using a quite different analytical approach. With the advances of self-assembled techniques, nanoscopic semiconductor rings were fabricated recently with a characteristic inner/outer radius of 10/30-70 nm and 2-3 nm in height^{6,7}. After the successful experimental realizations, additional effects, such as finite width^{8,9}, presence of barriers¹⁰, and penetration of the magnetic field into ring region¹¹, on the excitonic levels were also taken into account theoretically.

Very recently, Mano *et al.*¹² successfully demonstrated the formation of concentric quantum double rings with high uniformity and excellent rotational symmetry. The diameters of the inner and outer rings are 45 (± 3)nm and 100 (± 5)nm, respectively. Electronic structures of the concentric quantum double rings are then calculated theoretically.¹³ Motivated by these reports, we thus propose in this work a theoretical model to study the AB effect in concentric quantum double rings. The behavior of the AB oscillations in the double ring will be shown to depend on the positions and strengths of the coulomb impurities.

The model. —Consider now an electron in a two-dimensional concentric double ring with the inner ring shell enclosing a uniform static magnetic flux ($\Phi_B = B\pi r_a^2$) oriented along the z axis. The concentric double ring structure is approximated by the hard-wall con-

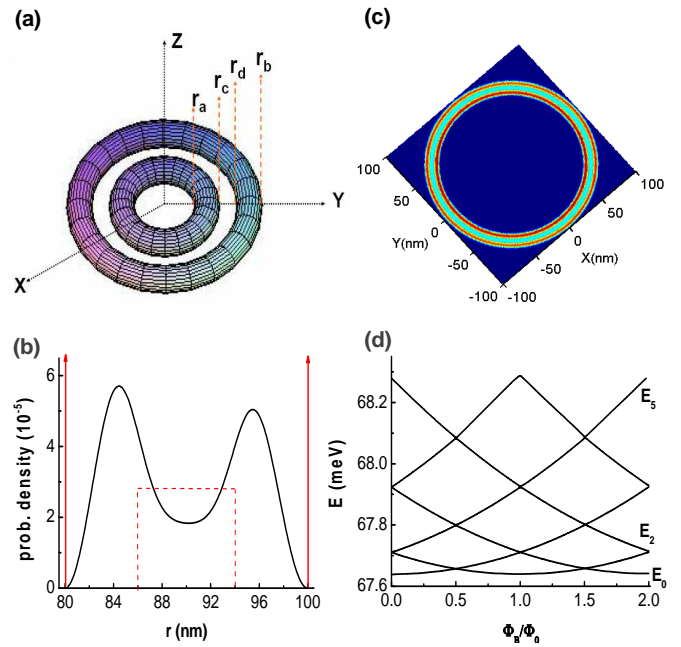


FIG. 1: (a) Illustration of the concentric quantum double ring. (b) Model potential of the concentric quantum double ring and the corresponding ground state wavefunction for an electron in the radial direction. (c) The probability density of the ground state electron. (d) Energy levels as a function of the magnetic flux Φ_B threading through the interior of the double rings.

finement potential with a tunable constant barrier in the middle as shown in Fig. 1 (b). The model Hamiltonian can be written as

$$H = \frac{(\vec{P} + \frac{e\vec{A}}{c})^2}{2m_e^*} + V(r), \quad (1)$$

where \vec{P} is canonical momentum, \vec{A} is the magnetic vector potential, and m_e^* is the effective mass of the electron.

The potential V is then defined as

$$V(r) = \begin{cases} \infty, & \text{if } r < r_a, r > r_b \\ V_0, & \text{if } r_c < r < r_d \\ 0 & \text{otherwise} \end{cases}. \quad (2)$$

The Hamiltonian operator inside the ring is

$$\hat{H} = \frac{\hat{P}_r^2}{2m_e^*} + \frac{(\hat{P}_\phi + \frac{eA_\phi}{c})^2}{2m_e^*} + V_0. \quad (3)$$

The vector potential needed to produce the magnetic field \vec{B} ($= B\hat{z}$) in the interior of the double ring is $\vec{A} = \frac{Br^2}{2r}\hat{\phi}$. The position representation of Eq. (3) can be written as

$$H = -\frac{\hbar}{2m_e^*} \left(\frac{d^2}{dr^2} + \frac{1}{r} \frac{d}{dr} \right) - \frac{\hbar^2}{2m_e^* r^2} \left(\frac{\partial}{\partial \phi} + \frac{e\Phi_B}{2\pi\hbar c} \right)^2 + V_0. \quad (4)$$

As is well known, the wave function $\psi_{n,m}(r, \phi)$ (n, m denote the principal and the magnetic quantum number, respectively) of the electron in the single ring is given by

$$\psi_{n,m}(r, \phi) = [C_1 J_{|m|}(kr) + C_2 Y_{|m|}(kr)] \cdot \left(\frac{1}{\sqrt{2\pi}} e^{im\phi} \right), \quad (5)$$

where C_1 and C_2 are the normalization constants. To solve the double ring problem, $\psi_{n,m}$ is chosen as the complete set to span the Hamiltonian operator. The energy eigenvalues E_j and the corresponding eigenfunctions $|\Phi_j\rangle$ can then be obtained via numerical diagonalization of \hat{H} in the matrix representation. In our calculations, the effective Rydberg unit, $Ry^* = m_e^* e^4 / 2\hbar^2 (4\pi\epsilon_0\epsilon_r)^2 = 5.8meV$, is adopted. The unit in length is effective Bohr radius, $a_B^* = 4\pi\epsilon_0\epsilon_r\hbar^2 / m_e^* e^2 = 10nm$. The effective mass of the electron is $0.067m_e$, and the universal flux quanta Φ_0 for a radius of a_B^* corresponds to a magnetic field of $13.18T$ in $GaAs/Al_{0.3}Ga_{0.7}$. The boundaries of the double rings are chosen as

$$\begin{cases} r_a = 80nm(8a_B^*) \\ r_b = 100nm(10a_B^*) \\ r_c = 86nm(8.6a_B^*) \\ r_d = 94nm(9.4a_B^*) \end{cases} \quad (6)$$

with the middle barrier $V_0 = 100meV$, which makes the tunneling between two rings become possible.

Fig. 1. (c) and (d) show respectively the probability density of the ground state and the energy spectra of the electron in the presence of magnetic flux Φ_B . Just like the behavior in single ring, the AB effect is clearly seen whenever $\frac{\Phi_B}{\Phi_0}$ ($\Phi_0 \equiv \frac{hc}{e}$ is the universal magnetic quantum) is a positive integer.

Effects of fixed impurities. —Let us now consider a positively charged impurity located at the inner ring ($r_i = 83nm, \phi_i = 0$) of a concentric quantum double ring. The potential between the electron and impurity can be described by the screened coulomb (Debye) potential¹⁴

$$U = \frac{-e^2 \cdot e^{-\alpha|\vec{r}_e - \vec{r}_i|}}{\epsilon_r |\vec{r}_e - \vec{r}_i|}, \quad (7)$$

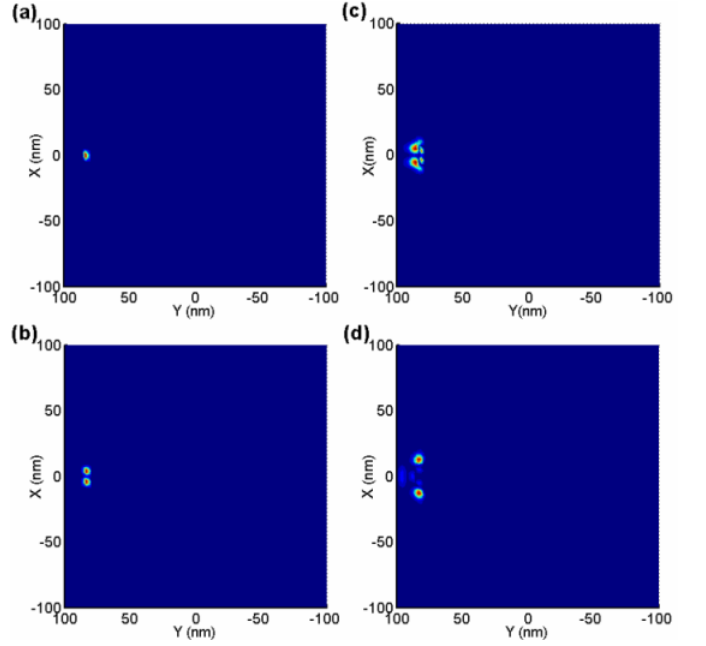


FIG. 2: Density plot of the electron wavefunction in the (a) ground state (E_0); (b) second excited state (E_2); (c) fifth excited state (E_5); (d) ninth excited state (E_9).

where the ϵ_r is the static dielectric constant (for GaAs, $\epsilon_r = 12.4$) and α is the screening parameter. Let us first consider the case of bared coulomb potential, i.e. $\alpha = 0$. Probability densities of the electron for various quantum states are shown in Fig. 2. As can be seen, even for the ninth excited state (E_9), the wavefunction that penetrates into the outer ring is still few.

Unlike the AB behavior in Fig. 1, the total energy (E_t) of the electron in the low quantum state increases monotonically with the increasing of the magnetic flux as shown in Fig. 3 (a) and (b). The reason is that the bared coulomb potential is so strong, such that it's almost impossible for the electron to circle around the ring. However, for the case without the impurity, the kinetic energies (E_k) in Fig. 1 do show the AB oscillation. From the definition of binding energy, $-E_b = E_t - E_k$, the AB oscillation can be revealed as one plots the variations of binding energy in Fig. 3 (c) or (d). One also notes that the binding energy of the second excited state (E_2) increases as the flux is increased from zero to half of Φ_0 . On the contrary, the binding energy of the fifth excited state (E_5) decreases first in the beginning. This tendency can also be understood from the combination of the two factors: the oscillatory kinetic energies in Fig. 1 (d) and the monotonically increasing behavior in Fig. 3 (a) and (b).

To see the effect of the screening parameter, it is convenient to define the parameter $\delta = \alpha a_B^*$, which contains no unit. Fig. 4 represents the probability densities of the ground state wavefunctions for different values of δ . As

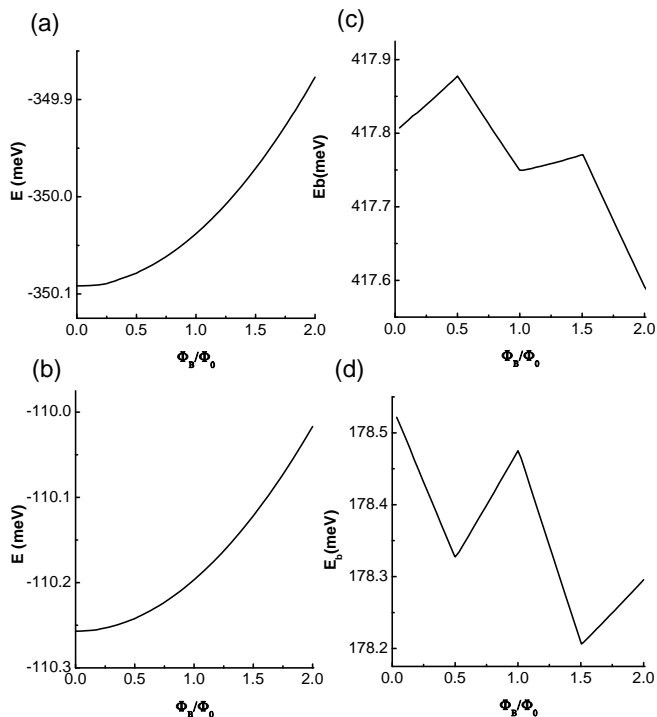


FIG. 3: (a) and (b) represent the total energies (E_t) of the second and fifth excited states, respectively. (c) and (d) show the corresponding binding energies (E_b), which exhibit AB oscillations, as functions of Φ_B .

can be seen, the probability density of the electron gathered around the position of the impurity when $\delta = 0.05$. As δ increases, the probability density of the electron begins to spread in the concentric quantum double ring. Since we are interested in the problem of impurity mixed with AB effect, we choose $\delta = 0.4$, for which the wavefunction spreads but not too much, in the rest of the discussions.

The energy spectra for the uniform magnetic flux threading the interior of the concentric double ring are shown in Fig. 5 (a). Since the coulomb potential is much weaker¹⁴, the AB effect can now be revealed in the spectra of total energy. Also, due to the fixed impurity, the cylindrical symmetry of the concentric double ring is broken and the two-folded energy degeneracies for each m ($m \neq 0$) are then removed. As a result, the AB effect is reduced in the presence of the fixed impurity. If one compares Fig. 5 (a) with Fig. 1 (d), the gaps are found to be opened at the points of intersecting curves in Fig. 1. (d), just like the band structures in solid state physics. This is because the magnetic flux, $2\pi\Phi_B/\Phi_0$, plays the same role as kL in one-dimensional Bloch problem¹⁵, where k is the wave vector and L is the length of the one dimensional lattice. The energy levels of the ring-formed microbands as a function of Φ_B are analogous to the Bloch electron bands in the extended k -zone picture.

If one further puts an additional impurity which is op-

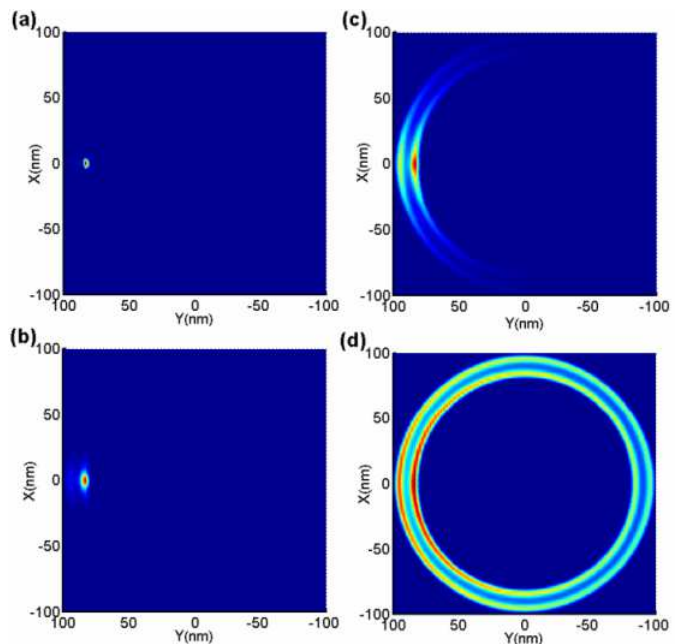


FIG. 4: Probability density of the ground state electron with a fixed impurity located at ($r_i = 83nm, \phi_i = 0$) in the concentric quantum double ring with (a) $\delta = 0.05$, (b) $\delta = 0.2$, (c) $\delta = 0.4$, and (d) $\delta = 0.6$.

posite to the first impurity in the inner ring, the degeneracies are removed further as shown in Fig. 5 (b), i.e. the separations of originally degenerate states (for example, E_7 and E_8) become bigger. However, since two impurities are symmetric, it also forces the degenerate states to intersect with another states (for example, E_6 and E_7). That's why the "energy gaps" look like disappear. The most important characteristic for concentric quantum rings is the inner and outer ring structure. One can move the second impurity to the middle of outer ring ($r = 97nm, \phi = \pi$). As shown in Fig. 5 (c), the energy gaps are opened again. The reason is that the wave functions are not symmetric with respect to the middle barrier V_0 [see Fig. 1. (c)]. Therefore, the attractive ability of the two impurities located at different rings are not the same. In addition, one can also suppress the azimuthal symmetry, i.e. locating the two impurities at the same ring (inner ring) but at different azimuthal angles ($\phi = 0, \frac{\pi}{2}$). As can be seen from Fig. 5 (d), the energy separations are larger than those for single impurity case, and the curves do not intersect with each other.

In summary, we have studied the AB effect in a concentric double ring. Effect of impurities with screened coulomb potential on the energy spectra is studied. The appearance of the AB oscillation in total energy is found to depend on the strength of the screened potential. In the case of screened potential, the openings and closings of the energy gaps depend not only on the angular distributions of the impurities, but also on whether the im-

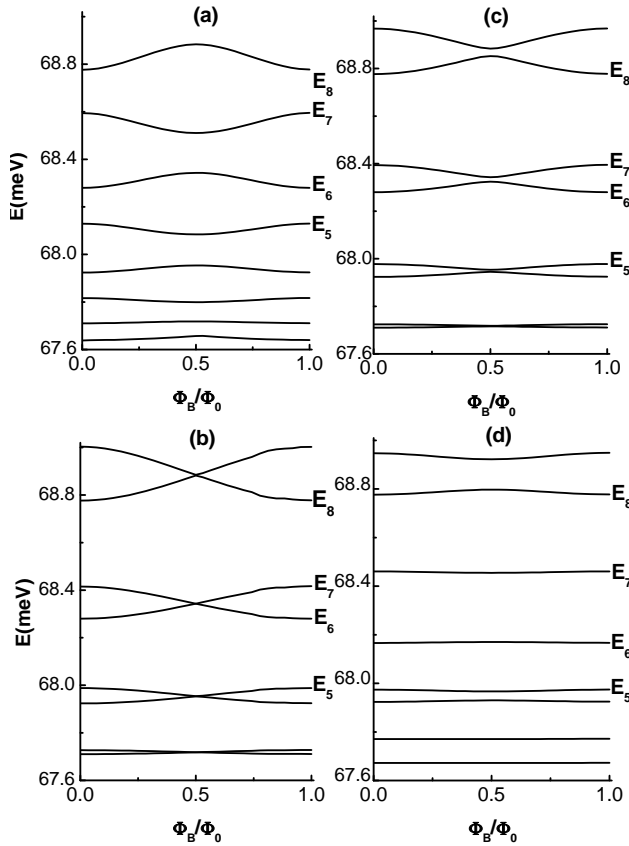


FIG. 5: Energy spectra as a function of the magnetic flux Φ_B with (a) a fixed impurity located at $(r_i = 83nm, \phi_i = 0)$; (b) two symmetric fixed impurities located at $(r_{i1} = 83nm, \phi_{i1} = 0)$ and $(r_{i2} = 83nm, \phi_{i2} = \pi)$; (c) two fixed impurities located at $(r_{i1} = 83nm, \phi_{i1} = 0)$ and $(r_{i2} = 97nm, \phi_{i2} = \pi)$; (d) two asymmetric fixed impurities located at $(r_{i1} = 83nm, \phi_{i1} = 0)$ and $(r_{i2} = 83nm, \phi_{i2} = \frac{\pi}{2})$.

purities are located at the same ring, which is the unique feature for the double ring systems.

ACKNOWLEDGMENTS

We thank Prof. Johnson Lee at Chung Yuan Christian University and Dr. W. H. Kuan at Center for Theoretical

Sciences for helpful discussions. This work is supported partially by the National Science Council, Taiwan under the grant number NSC 95-2119-M-009 -030.

* Electronic address: ynchen.ep87g@nctu.edu.tw

- [1] Y. Aharonov and D. Bohm, Phys. Rev. **115**, 485 (1959).
- [2] R. A. Webb, S. Washburn, C. P. Umbach, and R. B. Laibowitz, Phys. Rev. Lett. **54**, 2696 (1985).
- [3] Ho-Fai Cheung, Yuval Gefen, Eberhard K. Riedel, and Wei-Heng Shih, Phys. Rev. B **37**, 6050 (1988).
- [4] A. Chaplik, Pis'ma Zh. Èksp. Teor. Fiz. **62**, 885 (1995) [JETP Lett. **62**, 900 (1995)].
- [5] R. A. Römer and M. E. Raikh, Phys. Rev. B **62**, 7045 (2000).
- [6] A. Lorke and R. J. Luyken, Physica B **256-258**, 424 (1998); A. Lorke, R. J. Luyken, M. Fricke, J. P. Kotthaus, G. MedeirosRibeiro, J. M. Garcia, and P. M. Petroff, Microelectron. Eng. **47**, 95 (1999); H. Pettersson, R. p. J. Warburton, A. Lorke, K. Karrai, J. P. Kotthaus, J. M. Garcia, and P. M. Petroff, Physica E (Amsterdam) **6**, 510 (2000).
- [7] A. Lorke, R. J. Luyken, A. O. Govorov, J. P. Kotthaus, J. M. Garcia, and P. M. Petroff, Phys. Rev. Lett. **84**, 2223 (2000).
- [8] Jakyoungh Song and Sergio E. Ulloa, Phys. Rev. B **63**, 125302 (2001).
- [9] Hui Hu, Jia-Lin Zhu, Dai-Jun Li, and Jia-Jiong Xiong, Phys. Rev. B **63**, 195307 (2001).
- [10] Jia-Lin Zhu, Xiquan Yu, and Zhensheng Dai, Phys. Rev. B **67**, 075404 (2003).
- [11] O. Voskoboynikov, Yiming Li, Hsiao-Mei Lu, Cheng-Feng Shih, and C. P. Lee, Phys. Rev. B **66**, 155306 (2002).
- [12] Takaaki Mano, Takashi Kuroda, Stefano Sanguinetti, Tetsuyuki Ochiai, Takahiro Taten, Jongsu Kim, Takeshi Noda, Mitsuo Kawabe, Kazuaki Sakoda, Giyu Kido, and Nobuyuki Koguchi, Nano Lett. **5**, 425 (2005).
- [13] J. I. Climente, J. Planelles, M. Barranco, F. Malet, and M. Pi, Phys. Rev. B **73**, 235327 (2006); J. Planelles and J. I. Climente, Eur. Phys. J. **B 48**, 65 (2005); B. Szafran and F. M. Peeters, Phys. Rev. B **72**, 155316 (2005).
- [14] Y. P. Varshni, Superlattices and Microstructures, Vol. **29**, 233 (2001).
- [15] N. Byers and C. N. Yang, Phys. Rev. Lett. **7**, 46 (1961).